AD_____

Award Number:
W81 XWH-10-1-0740

TITLE:
Maintenance of epithelial stem cells by Cbl proteins

PRINCIPAL INVESTIGATOR:
Mayumi Naramura, M.D.

CONTRACTING ORGANIZATION:
University of Nebraska Medical Center
Omaha, Nebraska 68198

REPORT DATE:
September 2013

TYPE OF REPORT:
Final

PREPARED FOR: U.S. Army Medical Research and Materiel Command
                        Fort Detrick, Maryland 21702-5012

REPORT DOCUMENTATION PAGE

Form Approved
OMB No. 0704-0188

Public reporting burden for this collection of information is estimated to average 1 hour per response, including the time for reviewing instructions, searching existing data sources, gathering and maintaining the data needed, and completing and reviewing this collection of information. Send comments regarding this burden estimate or any other aspect of this collection of information, including suggestions for reducing this burden to Department of Defense, Washington Headquarters Services, Directorate for Information Operations and Reports (0704-0188), 1215 Jefferson Davis Highway, Suite 1204, Arlington, VA 22202-4302. Respondents should be aware that notwithstanding any other provision of law, no person shall be subject to any penalty for failing to comply with a collection of information if it does not display a currently valid OMB control number. **PLEASE DO NOT RETURN YOUR FORM TO THE ABOVE ADDRESS.**

1. REPORT DATE September 2013	2. REPORT TYPE Final	3. DATES COVERED 1 September 2010 – 31 August 2013
4. TITLE AND SUBTITLE Maintenance of Epithelial Stem Cells by Cbl Proteins		5a. CONTRACT NUMBER
		5b. GRANT NUMBER W81XWH-10-1-0740
		5c. PROGRAM ELEMENT NUMBER
6. AUTHOR(S) Mayumi Naramura E-Mail: mnaramura@unmc.edu		5d. PROJECT NUMBER
		5e. TASK NUMBER
		5f. WORK UNIT NUMBER
7. PERFORMING ORGANIZATION NAME(S) AND ADDRESS(ES) University of Nebraska Medical Center 987835 Nebraska Medical Center Omaha, Nebraska 68198-6810		8. PERFORMING ORGANIZATION REPORT NUMBER
9. SPONSORING / MONITORING AGENCY NAME(S) AND ADDRESS(ES) U.S. Army Medical Research and Materiel Command Fort Detrick, Maryland 21702-5012		10. SPONSOR/MONITOR'S ACRONYM(S)
		11. SPONSOR/MONITOR'S REPORT NUMBER(S)

12. DISTRIBUTION / AVAILABILITY STATEMENT
Approved for Public Release; Distribution Unlimited

13. SUPPLEMENTARY NOTES

14. ABSTRACT

The Cbl family E3 ubiquitin ligases are critical regulators of tyrosine kinase-mediated signal transduction, and we and others demonstrated that the Cbl family proteins were required to maintain the homeostasis of the hematopoietic stem cell compartment and disturbance of this critical regulatory pathway led to cancer in human and mice. However, their roles in the epithelial stem/progenitor cells has never been examined. Using the newly-established, in vitro-differentiating hTERT-immortalized human mammary epithelial cell (hMEC) line, we demonstrated that loss of Cbl inhibited differentiation of epithelial cells. Our preliminary studies indicate that Cbl functions in multiple signaling pathways beyond the traditional EGFR-MEK-Erk pathway, which led to the complex phenotypes of Cbl deficiency in the epithelial compartment. Data from genetically-modified mouse models support that loss of Cbl and Cbl-b in the mammary epithelial compartment decreases the size of the stem/progenitor compartment and inhibits normal differentiation. Thus, unlike hematopoietic system, Cbl proteins are required for the survival and normal differentiation of mammary epithelial cells. These data highlight the tissue specificity of signal transduction pathways.

15. SUBJECT TERMS
breast cancer, mammary epithelial stem cells, Cbl, ubiquitin ligase

16. SECURITY CLASSIFICATION OF:			17. LIMITATION OF ABSTRACT	18. NUMBER OF PAGES	19a. NAME OF RESPONSIBLE PERSON USAMRMC
a. REPORT U	b. ABSTRACT U	c. THIS PAGE U	UU	42	19b. TELEPHONE NUMBER *(include area code)*

Table of Contents

Introduction

Gene expression analyses identified several subtypes of breast cancer which show distinct prognosis and responses to treatment [1]. It is now widely accepted that these different subtypes originate from breast epithelial cells at distinct developmental stages [2, 3]. Therefore, in order to determine the origin of breast cancer and apply such knowledge to improve prevention, diagnosis and treatment, it is imperative to fully understand the molecular mechanisms of normal mammary gland development. The Cbl family E3 ubiquitin ligases, Cbl, Cbl-b and Cbl3 in mammals, are critical regulators of tyrosine kinase-mediated signal transduction [4], and we and others demonstrated that Cbl family proteins were required for the maintenance of the hematopoietic stem cell homeostasis [5-7]. Loss of function of this critical regulatory pathway led to cancer in human and mice. However, the role of the Cbl family proteins in the epithelial stem/progenitor cells has never been examined directly. Tyrosine kinase-mediated signaling, which is regulated by Cbl family proteins, is known to play prominent roles in mammary gland development. Therefore, we formed a hypothesis that Cbl family proteins are required for the maintenance of stem/progenitor homeostasis in the mammary epithelium, and that loss of this regulatory control will enlarge the stem/progenitor pool and predispose the mammary gland to oncogenesis. To test this hypothesis, we proposed to employ two complementary approaches, one involving the use of a newly-established hTERT-immortalized human mammary epithelial cell (hMEC) line (hereafter called $K5^+ K19^-$ hMEC) [8], and the gene knock-out mouse strains.

Body

In order to test the hypothesis above, we proposed following Specific Aims:

Aim 1. Define the role of the Cbl family protein in progenitor-type mammary epithelial cells in culture

Aim 2. Define the role of the Cbl family proteins in mammary gland development and tumorigenesis in vivo.

and following specific tasks were identified:

Task 1: Define the role of the Cbl family proteins in progenitor-type mammary epithelial cells in culture (Months 1-18)

1-a. Establish the base line for flow cytometry markers and flow-based functional analyses (Hoechst dye exclusion, ALDEFLUOR assay) (Months 1-6)

1-b. Establish mammosphere culture and differentiation assay conditions for progenitor-type MEC lines (Months 4-9)

1-c. Generate Cbl/Cbl-b double deficient human progenitor MEC lines using shRNA (Months 7-12)

1-d. Characterize control and Cbl/Cbl-b double deficient MECs by flow cytometry and functional analyses (Months 13-24)

Task 2: Define the biochemical pathways affected by Cbl/Cbl-b loss by microarray analyses (Months 13-24)

2-a. Perform microarray analyses on control and Cbl/Cbl-b double deficient MECs growing in nondifferentiating conditions (Months 13-18)

2-b. Perform microarray analyses on control and Cbl/Cbl-b double deficient MECs undergoing lineage differentiation (Months 19-24)

Task 3: Define the role of the Cbl family proteins in mammary gland development and tumorigenesis in vivo (Months 1-24)

3-a. Generate sufficient number of MMTV-Cre;Cbl(flox/flox);Cblb(-/-) for

mammary gland transplant (Months 1-12)

3-b. Characterize transplanted mammary gland phenotypes by histology, immunohistochemistry and flow cytometry (Months 7-18)

3-c. Characterize transplanted mammary gland phenotypes by serial transplantation and tissue regeneration assay (Months 13-24)

Here we summarize our research findings during the entire grant period (Sept. 2010 – Aug. 2013).

1. Analysis of Cbl functions in progenitor-type mammary epithelial cells (K5$^+$ K19$^-$ hMEC) in culture

First, we established that K5$^+$ K19$^-$ hMEC can be reproducibly differentiated in culture. We monitored cell differentiation by morphology, immunofluorescence staining and flow cytometry. Data from these experiments are reported in Figure 1 of Mukhopadhyay et al. (Appendix 1)

In order to evaluate the effect of Cbl loss in this *in vitro* differentiating cell line model, we introduced tetracycline-inducible shRNAs against Cbl (2011 Report, Figure 4). Cbl shRNA expression induction in K5$^+$ K19$^-$ hMEC inhibited differentiation of MECs as determined by morphology and marker expression (2011 Report, Figure 5).

Because three members of the Cbl family proteins share high degrees of structural and functional similarities, Cbl-b and/or Cbl3 may have compensated for the loss of Cbl in Cbl shRNA-expressing cells. To address this, we introduced a tetracycline-inducible CblN construct which functions as a dominant negative inhibitor of all Cbl family proteins. Induction of CblN expression in K5$^+$ K19$^-$ hMEC inhibited differentiation of MECs, suggesting that Cbl family functions are required for in vitro differentiation of K5$^+$ K19$^-$ hMECs (Figure 1).

Based on these observations, we sought to investigate how Cbl regulates K5$^+$ K19$^-$ hMEC differentiation. Previous biochemical studies by us and others demonstrated that Cbl family proteins are critical negative regulators of tyrosine kinases such as EGFR. Essential roles of EGFR-mediated signals in normal mammary gland are apparent from phenotypes of amphiregulin (AREG, one of the EGFR ligands)-deficient mice [9] as well as *wa2* (naturally occurring *egfr* mutant) mice [10]; in both strains, mammary glands are morphologically and functionally underdeveloped. Therefore, we identified EGFR as a potential target of Cbl in this process and investigated effects of signaling through EGFR upon K5$^+$ K19$^-$ hMEC differentiation. Effects of three different EGFR ligands, EGF, AREG and TGFα have been reported in Mukhopadhyay et al (Appendix 1). In this paper, we demonstrated that sustained activation of the EGFR-MEK-ERK pathway led to preferential differentiation into myoepithelial lineage, whereas inhibition of the PI3K-Akt pathway accelerated MEC differentiation.

Cbl-deficient MECs showed sustained ERK activation when stimulated with EGF (2012 Report, Figure 3), as expected. This, however, did not lead to preferential differentiation into myoepithelial lineage. Furthermore, when K5$^+$ K19$^-$ hMECs were allowed to differentiate prior to expression of Cbl shRNA, only undifferentiated cells remained and differentiated cells died (Figure 2), indicating Cbl expression is required for survival of differentiated K5$^+$ K19$^-$ hMECs.

Clearly, lack of K5$^+$ K19$^-$ hMEC differentiation in the absence of Cbl activity cannot be accounted for by the changes in the EGFR-MEK-ERK-dependent pathway.

To address these paradoxical findings, we investigated the effect of Cbl loss on the Akt pathway and found that Cbl-deficient K5$^+$ K19$^-$ hMECs showed prolonged activation of Akt (2012 Report, Figure 6). This is consistent with previously-reported roles of Cbl as a negative regulator of the PI3 kinase-Akt pathway. In light of our observations that inhibition of the PI3K-Akt pathway led to accelerated differentiation of K5$^+$ K19$^-$ hMECs, we consider that the observed phenotypes in Cbl-deficient K5$^+$ K19$^-$ hMECs may be due to prolonged activation of Akt.

Among various downstream effectors of the Akt pathway, GSK-3 beta is a ubiquitously expressed serine/threonine protein kinase whose activity can be inhibited by Akt-mediated phosphorylation at Ser9. Active GSK3 phosphorylates beta catenin and promotes its degradation. Thus, inhibition of GSK3 activity, i.e., increased phosphorylation at Ser9, is linked to stabilization of beta catenin. While phosphorylation of beta catenin by GSK3 is a signal for destabilization, phosphorylation of this protein at Ser552 is known to induce protein accumulation, nuclear transport and subsequent elevation of the transcriptional activity. As shown in Figure 6 in 2012 Report, phosphorylation of GSK3 beta at Ser9 (inactivating phosphorylation) and that of beta catenin at Ser552 (activating phosphorylation) was enhanced in Cbl knock-down TERT-hMECs. Because enhanced beta catenin activity is associated with stem cell maintenance in various systems, we consider that the activation of the beta catenin pathway may be a potential mechanism behind inhibition of MEC differentiation in the absence of Cbl.

In conclusion, we determined that Cbl is required for in vitro differentiation of K5$^+$ K19$^-$ hMECs. Existing evidence is consistent with the idea that Cbl regulates K5$^+$ K19$^-$ hMEC differentiation through the PI3K-Akt-GSK3-beta catenin pathway, but further investigation is required to establish this.

2. Analysis of Cbl functions in vivo using gene mutant mouse models
We originally proposed to analyze the effect of simultaneous loss of Cbl and Cbl-b in the mouse mammary gland using MMTV-Cre;Cbl(flox/flox);Cblb(-/-) mice. Because MMTV-Cre;Cbl(flox/flox);Cblb(-/-) mice succumb to hematopoietic disorders within 2 to 3 months after birth due to MMTV-Cre activation in the small subset of hematopoietic stem cells [6], we transplanted mammary tissue from the control and MMTV-Cre;Cbl(flox/flox);Cblb(-/-) mice into the cleared fat pads of immunodeficient NSG females. Cbl, Cbl-b double deficient mouse MECs produced fewer branching and they were less efficient at filling the recipient's fat pads than control MECs (2011 Report, Figure 6). When the surface markers were analyzed by flow cytometry, Lineage$^-$ CD29^{hi}, CD24$^+$ fraction, which is enriched for multipotent mammary epithelial stem cells, was reduced compared to controls (2011 Report, Figure 7).

Of note, the MMTV-Cre;Cbl(flox/flox);Cblb(-/-) mice still express Cbl3. When evaluated the expression levels of three Cbl family members in various mammary epithelial cell compartments, we found all members are expressed (Figure 3). Therefore, we identified a need to evaluate the triple knock-out (Cbl, Cbl-b and Cbl3 knock-out) in order to fully understand the role of Cbl family proteins in the mammary gland development. Because simultaneous loss of

Cbl and Cbl-b in the germline is not compatible with embryonic development, mammary epithelial cells from Cbl(flox/flox); Cblb(-/-); Cblc(-/-) mice will be useful for this purpose.
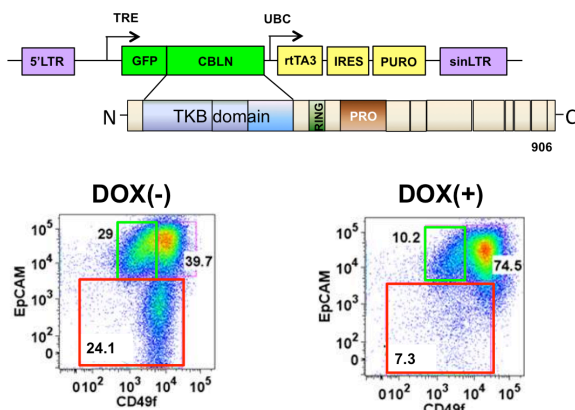

Figure 1. CblN expression inhibits differentiation of K5$^+$ K19$^-$ hMECs. Doxycycline-inducible CblN (N-terminal truncated product of Cbl; functions as a dominant-negative mutant) was introduced to K5$^+$ K19$^-$ hMECs. Cells were subjected to differentiation condition and analyzed by flow cytometry. The bottom panels show that the proportion of luminal cells (EpCAM^{hi} CD49f^{med}) decreased from 29 to 10.2%, and that of myoepithelial cells (EpCAM^{lo}) decreased from 24.1 to 7.3 % when CblN was expressed during in vitro differentiation.
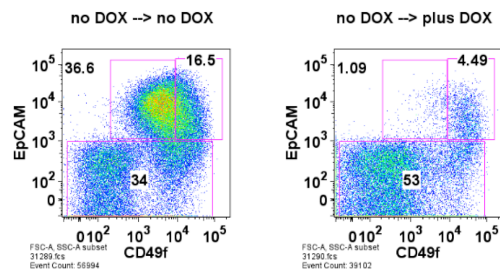

Figure 2. Cbl is required for survival of differentiation K5$^+$ K19$^-$ hMECs. Cells carrying inducible shRNA against Cbl were differentiated in the absence of doxycycline (i.e., with normal levels of Cbl expression). Three weeks after the initiation of in vitro differentiation, when cells have visibly differentiated, Cbl shRNA expression was induced. Cbl shRNA expression reduced the proportion of luminal cells (EpCAM^{hi} CD49f^{med}) from 36.6 to 1.09%.
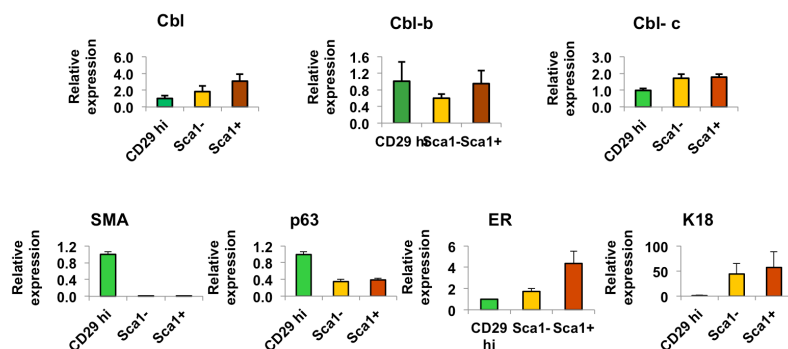

Figure 3. Expression levels of Cbl family gene products in primary mouse mammary epithelial cells. Primary mammary epithelial cells from virgin adult (8 weeks) female mice were sorted based on the surface marker expression (CD29^{hi}, stem and myoepithelial; CD24^{hi} Sca1^{lo}, luminal progenitor; CD24^{hi} Sca1^{hi}, mature luminal) and transcript levels were determined by quantitative RT-PCR. Smooth muscle actin (SMA), p63, estrogen receptor (ER) and cytokeratin 18 (K18) were evaluated simultaneously to confirm identity of each population.

Key Research Accomplishments
- Established in vitro cell differentiation assay of K5$^+$ K19$^-$ hMECs.
- Established K5$^+$ K19$^-$ hMECs expressing tetracycline-inducible shRNA against Cbl.
- Established K5$^+$ K19$^-$ hMECs expressing tetracycline-inducible CblN (dominant-negative inhibitor of Cbl).
- Demonstrated that inhibition of Cbl functions either by expressing Cbl shRNA or CblN blocks the differentiation of K5$^+$ K19$^-$ hMECs in vitro.
- Demonstrated that various EGFR ligands exert distinct effects on the differentiation of K5$^+$ K19$^-$ hMECs and showed that this effect is, at least in part, mediated by the EGFR-MEK-Erk pathway (Mukhopadhyay et al., PLOS ONE, in press)
- Demonstrated that the mammary gland development is altered in MMTV-Cre; Cbl(flox/flox); Cblb(-/-) mice
- Evaluated expression levels of three Cbl family gene products (Cbl, Cblb and Cbl3) in various mammary epithelial compartments

Reportable Outcomes

Manuscripts, abstracts, presentations are listed under Bibliography

Funding
- Skala Fellowship awarded to Chandrani Mukhopadhyay (graduate student in the lab)

Development of cell lines and animal models:
- K5$^+$ K19$^-$ hMECs with inducible human Cbl shRNA
- K5$^+$ K19$^-$ hMECs with inducible dominant negative mutant Cbl (CblN)
- Established mouse mammary epithelial cell culture, virus infection and transplantation

Conclusions
In this DOD-funded project, we demonstrated that Cbl family proteins play critical roles in mammary epithelial cell physiology. This is the first time that the role of Cbl proteins was directly demonstrated in biologically-relevant mammary epithelial cell systems. Specifically,

1. We established that the K5$^+$ K19$^-$ hMECs faithfully reproduced numerous key aspects of normal human mammary epithelial cell differentiation, thus validated them as a tractable in vitro model of this complex system. In light of data linking breast cancer cells of origin with various developmental stages of mammary epithelial cells, precise knowledge into regulatory mechanisms of mammary gland development is essential for devising effective prevention/early detection strategies of breast cancer.

2. Using this newly-defined system, we showed that loss of Cbl interferes with differentiation of K5$^+$ K19$^-$ hMECs. Biochemically, this phenotype is not mediated by the EGFR-MEK-Erk pathway. We consider Cbl-dependent regulation of the PI3K-Akt pathway as a candidate responsible for the observed phenotypes, but further experiments are required to establish this.

3. In parallel with the in vitro cell line model, we used genetically-modified mouse models to show that Cbl proteins are required to maintain normal development of the mammary gland. In contrast to the hematopoietic system, where the loss of Cbl proteins led to enlargement of the

stem/progenitor compartments and resulted in pathological expansion of the myeloid lineage, loss of Cbl proteins (Cbl and Cbl-b) did not enlarge the stem/progenitor compartment, nor accelerate mammary epithelial cell growth. These data collectively show the tissue specificity of signal transduction regulation, and highlight the needs for performing investigation in biologically relevant systems.

References
1.   Sørlie T, Perou CM, Tibshirani R, Aas T, Geisler S, Johnsen H, Hastie T, Eisen MB, van de Rijn M, Jeffrey SS, Thorsen T, Quist H, Matese JC, Brown PO, Botstein D, Eystein Lønning P, et al. Gene expression patterns of breast carcinomas distinguish tumor subclasses with clinical implications. Proc. Natl. Acad. Sci. U.S.A. 2001; 98: 10869-10874.
2.   Visvader JE. Cells of origin in cancer. Nature. 2011; 469: 314-322.
3.   Molyneux G, Smalley MJ. The cell of origin of BRCA1 mutation-associated breast cancer: a cautionary tale of gene expression profiling. J Mammary Gland Biol Neoplasia. 2011; 16:51-5.
4.   Duan L, Reddi AL, Ghosh A, Dimri M, Band H. The Cbl family and other ubiquitin ligases: destructive forces in control of antigen receptor signaling. Immunity. 2004; 21: 7-17.
5.   Rathinam C, Thien CBF, Langdon WY, Gu H, Flavell RA. The E3 ubiquitin ligase c-Cbl restricts development and functions of hematopoietic stem cells. Genes Dev. 2008; 22: 992-997.
6.   Naramura M, Nandwani N, Gu H, Band V, Band H. Rapidly fatal myeloproliferative disorders in mice with deletion of Casitas B-cell lymphoma (Cbl) and Cbl-b in hematopoietic stem cells. Proc. Natl. Acad. Sci. U.S.A. 2010; 107: 16274-16279.
7.   Rathinam C, Thien CBF, Flavell RA, Langdon WY. Myeloid leukemia development in c-Cbl RING finger mutant mice is dependent on FLT3 signaling. Cancer Cell. 2010; 18: 341-352.
8.   Zhao X, Malhotra GK, Lele SM, Lele MS, West WW, Eudy JD, Band H, Band V. Telomerase-immortalized human mammary stem/progenitor cells with ability to self-renew and differentiate. Proc. Natl. Acad. Sci. U.S.A. 2010; 107: 14146-14151.
9.   Luetteke NC, Qiu TH, Fenton SE, Troyer KL, Riedel RF, Chang A, Lee DC. Targeted inactivation of the EGF and amphiregulin genes reveals distinct roles for EGF receptor ligands in mouse mammary gland development. Development. 1999 Jun;126(12):2739-50.
10.   Fowler KJ, Walker F, Alexander W, Hibbs ML, Nice EC, Bohmer RM, Mann GB, Thumwood C, Maglitto R, Danks JA, Chetty R, Burgess AW, Dunn AR. A mutation in the epidermal growth factor receptor in waved-2 mice has a profound effect on receptor biochemistry that results in impaired lactation. Proc Natl Acad Sci U S A. 1995 Feb 28;92(5):1465-9.

Bibliography
Manuscripts, abstracts, presentations:
   Peer-reviewed research articles:
     • Duan L, Raja SM, Chen G, Virmani S, Williams SH, Clubb RJ, Mukhopadhyay C, Rainey MA, Ying G, Dimri M, Chen J, Reddi AL, **Naramura M**, Band V, Band H. Negative regulation of EGFR-Vav2 signaling axis by Cbl ubiquitin ligase controls EGF receptor-mediated epithelial cell adherens junction dynamics and cell migration. **J Biol Chem.** 2011 Jan 7;286(1):620-33. Epub 2010 Oct 12. PubMed PMID: 20940296; PubMed Central PMCID: PMC3013022.

- George M*, Rainey MA, **Naramura M***, Foster KW, Holzapfel MS, Willoughby LL, Ying G, Goswami RM, Gurumurthy CB, Band V, Satchell SC, Band H*. Renal thrombotic microangiopathy in mice with combined deletion of endocytic recycling regulators EHD3 and EHD4. **PLoS One.** 2011 Mar 9;6(3):e17838. PubMed PMID: 21408024; PubMed Central PMCID: PMC3052385. (*corresponding authors).

- Ortega-Cava C, Raja SM*, Laiq Z, Bailey TA, Luan H, Mohapatra B, Williams ST, Ericsson AC, Goswami R, Dimri M, Duan L, Band V, **Naramura M***, Band H*. Continuous requirement of ErbB2 kinase activity for loss of cell polarity and lumen formation in a novel ErbB2/Neu-driven murine cell line model of metastatic breast cancer. **J Carcinog**. 2011 10:29. PubMed PMID: 22190871. (*corresponding authors).

- Mohibi S, Gurumurthy CB, Nag A, Wang J, Mirza S, Mian Y, Quinn M, Katafiasz B, Eudy J, Pandey S, Guda C, **Naramura M,** Band H, Band V. Mammalian alteration/deficiency in activation 3 (Ada3) is essential for embryonic development and cell cycle progression. **J Biol Chem**. 2012 Aug 24;287(35)29442-56. PubMed PMID: 22736770.

- Helikar T, Kochi N, Kowal B, Dimri M, **Naramura M**, Raja SM, Band V, Band H, Rogers JA. A comprehensive, multi-scale dynamical model of ErbB receptor signal transduction in human mammary epithelial cells. PLoS One. 2013 Apr 18;8(4):e61757. doi: 10.1371/journal.pone.0061757. Print 2013. PubMed PMID: 23637902; PubMed Central PMCID: PMC3630219.

- Mukhopadhyay C, Zhao X, Maroni D, Band V, **Naramura M**. Distinct effects of EGFR ligands on human mammary epithelial cell differentiation. PLoS One. 2013 in press.

Review articles:
- Tu C, Ahmad G, Mohapatra B, Bhattacharyya S, Ortega-Cava CF, Chung BM, Wagner KU, Raja SM, **Naramura M**, Band V, Band H. ESCRT proteins: Double-edged regulators of cellular signaling. **Bioarchitecture.** 2011 Jan;1(1):45-48. PubMed PMID: 21866262; PubMed Central PMCID: PMC3158637.

- **Naramura M**, Nadeau S, Mohapatra B, Ahmad G, Mukhopadhyay C, Sattler M, Raja SM, Natarajan A, Band V, Band H. Mutant Cbl proteins as oncogenic drivers in myeloproliferative disorders. **Oncotarget.** 2011 Mar;2(3):245-50. PubMed PMID: 21422499; PubMed Central PMCID: PMC3134300.

- **Naramura M**, Band V, Band H. Indispensable roles of mammalian Cbl family proteins as negative regulators of protein tyrosine kinase signaling: Insights from in vivo models. **Commun Integr Biol.** 2011 Mar;4(2):159-62. PubMed PMID: 21655429; PubMed Central PMCID: PMC3104568.

- Bailey TA, Luan H, **Naramura M**, Band V, Raja SM, Band H. Mechanisms of trastuzumab resistance in ErbB2-driven breast cancer and newer opportunities to overcome therapy resistance. **J Carcinog**. 2011 10:28. PubMed PMID: 22190870.

- Nadeau S, An W, Palermo N, Feng D, Ahmad G, Dong L, Borgstahl GEO, Natarajan A, **Naramura M**, Band V, Band H. Oncogenic Signaling by Leukemia-Associated Mutant Cbl Proteins. **Biochem Anal Biochem.** 2012 S6-001. doi:10.4172/2161-1009.S6-001.

- Mohapatra B, Band H, Ahmad G, Nadeau S, Zutshi N, An W, Scheffee S, Dong L, Feng D, Goetz B, Borgstahl G, Natarajan A, Raja S, Naramura M, Band V, Arya P. Protein tyrosine kinase regulation by ubiquitination: critical roles of Cbl-family ubiquitin ligases. **Biochim Biophys Acta.** 2013 Jan;1833(1):122-39.

Book chapters
- **Naramura M**. 2012. Regulation of Tyrosine Kinase Signaling by Cbl in Hematopoietic Stem Cells *in* HEMATOPOIETIC STEM CELLS. R. Pelayo Camacho, Editor, InTech Open Access Publisher, Rijeka, Croatia. ISBN 978-953-307-746-8.

Presentations
- 2011 Midwest Student Biomedical Research Forum (Omaha, NE)
- 2011 Era of Hope (Orlando, FL)
- 2012 Midwest Student Biomedical Research Forum (Omaha, NE)
- 2012 Gordon Research Conference on Mammary Gland Biology (Lucca (Barga), Italy)
- 2012 Cold Spring Harbor Laboratory Meeting on Mechanisms and Models of Cancer (Cold Spring Harbor, NY)

List of personnel receiving pay from this research effort:
- Mayumi Naramura
- Vimla Band
- Chandrani Mukhopadhyay
- Matthew Storck
- Dulce Maroni

Appendix
1.   Mukhopadhyay C, Zhao X, Maroni D, Band V, Naramura M. Distinct effects of EGFR ligands on human mammary epithelial cell differentiation. PLoS One. 2013 in press.

Distinct effects of EGFR ligands on human mammary epithelial cell differentiation

Chandrani Mukhopadhyay[1], Xiangshan Zhao[2], Dulce Maroni[1], Vimla Band[1,2], Mayumi Naramura[1,2]

[1]Eppley Institute for Research in Cancer and Allied Diseases, University of Nebraska Medical Center, Omaha, Nebraska, United States of America

[2]Department of Genetics, Cell Biology and Anatomy, College of Medicine, University of Nebraska Medical Center, Omaha, Nebraska, United States of America

Chandrani Mukhopadyay: cmukhopa@unmc.edu

Xiangshan Zhao: xzhao@unmc.edu

Dulce Maroni: dmaroni@unmc.edu

Vimla Band: vband@unmc.edu

Mayumi Naramura: mnaramura@unmc.edu, corresponding author

Abstract

Based on gene expression patterns, breast cancers can be divided into subtypes that closely resemble various developmental stages of normal mammary epithelial cells (MECs). Thus, understanding molecular mechanisms of MEC development is expected to provide critical insights into initiation and progression of breast cancer.

Epidermal growth factor receptor (EGFR) and its ligands play essential roles in normal and pathological mammary gland. Signals through EGFR is required for normal mammary gland development. Ligands for EGFR are over-expressed in a significant proportion of breast cancers, and elevated expression of EGFR is associated with poorer clinical outcome.

In the present study, we examined the effect of signals through EGFR on MEC differentiation using the human telomerase reverse transcriptase (h$TERT$)-immortalized human stem/progenitor MECs which express cytokeratin 5 but lack cytokeratin 19 (K5$^+$K19$^-$ hMECs). As reported previously, these cells can be induced to differentiate into luminal and myoepithelial cells under appropriate culture conditions.

K5$^+$K19$^-$ hMECs acquired distinct cell fates in response to EGFR ligands epidermal growth factor (EGF), amphiregulin (AREG) and transforming growth factor alpha (TGFα) in differentiation-promoting MEGM medium. Specifically, presence of EGF during *in vitro* differentiation supported development into both luminal and myoepithelial lineages, whereas cells differentiated only towards luminal lineage when EGF was replaced with AREG. In contrast, substitution with TGFα led to differentiation only into myoepithelial lineage. Chemical inhibition of the MEK-Erk pathway, but not the phosphatidylinositol 3-kinase (PI3K)-AKT pathway, interfered with K5$^+$K19$^-$ hMEC differentiation.

The present data validate the utility of the K5$^+$K19$^-$ hMEC cells for modeling key features of human MEC differentiation. This system should be useful in studying molecular/biochemical mechanisms of human MEC differentiation.

Introduction

Molecular profiling of breast cancer revealed unexpected heterogeneity of this disease [1,2]. According to these studies, breast cancers can be categorized into several separate subtypes which share considerable similarities with various developmental stages of normal mammary epithelial cells (MECs). Consequently, a hypothesis was proposed that individual types of cancer might arise from malignant transformation of comparable normal MECs [3]; however, more recent studies employing lineage tracing [4–6], marker analysis [7], transplantation [8] and other techniques [7,9,10] began to uncover the complexity and the plasticity of the normal and pathological mammary epithelial developmental processes.

One of the difficulties of studying detailed molecular/biochemical mechanisms of normal and pathological MEC differentiation is the lack of accessible models. Sources of normal human MECs include reduction mammoplasty specimen and normal margins of surgically-excised tumor tissues, but primary cells have limited lifespan *in vitro*, and are not always readily available. Underlying genetic, epigenetic and environmental variations between donors may also be a concern. Genetically-engineered mouse models provide powerful tools to address important biological questions [11], but due to inherent differences between human and mouse mammary gland physiology, observations in mice may not directly translate to human pathophysiology. There are also technical challenges to follow developmental processes as they progress *in vivo*. To address these issues, Band and colleagues have previously established human telomerase reverse transcriptase (h*TERT*)-immortalized MEC lines that can be propagated indefinitely in a stem/progenitor-like undifferentiated state but can be induced to differentiate into luminal as well as myoepithelial lineages *in vitro* under defined conditions [12]. Because they are amenable to complex manipulations, these models should be useful for studying mechanisms of MEC self-renewal, differentiation, transformation and cancer progression.

In the present study, we sought to characterize and validate this cell line model further by focusing on the effects of signals through epidermal growth factor receptor (EGFR) on *in vitro* differentiation. EGFR is recognized as a critical regulator of mammary gland development [13]. A naturally-occurring mutation in the *egfr* gene in mice (*wa-2*) has been known to impair lactation [14]. On the ligand side, although multiple ligands are known to bind to EGFR, only amphiregulin (AREG)-deficient mice showed significant defects in the development of mammary gland, suggesting redundant as well as unique functions of individual EGFR ligands [15]. Links between the EGFR-dependent processes and mammary gland pathophysiology are further reinforced by the observations that EGFR is either amplified or overexpressed in a considerable proportion of basal-like breast cancers [16,17]; transcripts for EGFR ligands such as epidermal growth factor (EGF), AREG and transforming growth factor alpha (TGFα) are frequently upregulated in human breast cancer samples and a majority of breast cancers that express high levels of TGFα also co-express EGFR, suggesting a potential autocrine loop [18–22]. All these point towards the crucial roles of EGFR and its ligands in the biology of the mammary gland and breast cancer. As for the biochemical mechanisms, it was previously reported that sustained activation of the EGFR-MEK-Erk pathway was required for myoepithelial differentiation of primary human MECs [23]. Taking these prior observations into consideration, here we examined the effects of three EGFR ligands, EGF, AREG and TGFα in the differentiation-promoting MEGM medium on the h*TERT*-immortalized stem/progenitor hMEC line characterized by the presence of cytokeratin 5 and absence of cytokeratin 19 ($K5^+K19^-$ hMEC).

Materials and Methods

Cell culture

The development and initial characterizations of h*TERT*-immortalized stem/progenitor hMEC line defined by the presence of K5 and absence of K19 (K5$^+$K19$^-$ hMECs) were reported previously [12]. Cells were routinely maintained in the DFCI-1 medium [24]. All experiments were performed within 20 passages in culture.

For *in vitro* differentiation, K5$^+$K19$^-$ hMEC cells were cultured in MEGM medium (MEBM, (Lonza, Walkersville, MD, USA) supplemented with B27 (Life Technologies, Carlsbad, CA, USA), 4 µg/mL heparin (Sigma-Aldrich, St. Louis, MO, USA), 5 µg/mL insulin (Sigma-Aldrich), 30 ng/mL (5 nM) EGF (Life Technologies), 20 ng/mL FGF (Life Technologies) and 0.5 µg/ mL hydrocortisone (Sigma-Aldrich)). EGF was replaced with AREG or TGFα (5 nM unless specified otherwise) where indicated. Cells were passaged once a week and seeded at 2×10^5 in a 60 mm dish (for flow cytometry analysis) or 2×10^4 cells/well on the top of the 12 mm glass coverslip in the 24-well plate (for confocal imaging analysis).

Antibodies

Antibodies used for this study are listed in Table 1.

Immunofluorescence and confocal microscope image analysis

Immunofluorescence and confocal image analyses were performed as described previously [12]. Briefly, cells were grown on 12 mm glass coverslips, fixed with 4% paraformaldehyde in phosphate buffered saline (PBS) and permeabilized with 0.5% Triton X-100 for 5 minutes. After blocking non-specific binding sites with 5% goat serum for 1 hour, samples were incubated with the primary anti-K5 (1:2000) and anti-MUC1 (1:500) antibodies in 1% goat serum-containing PBS overnight at 4°C. After three washes with PBS, anti-rabbit IgG Alexa Fluor 488 and anti-mouse IgG Alexa Fluor 633 were added at 1:1000 dilutions in 1% goat serum containing PBS and incubated at room temperature for 1 hour. After washes in PBS and in water, nuclei were visualized with DAPI by mounting with VECTASHIELD Hard Set mounting medium (Vector Laboratories, Burlingame, CA). Images were captured with a Zeiss LSM 710 META laser scanning confocal microscope (Carl Zeiss Microscopy GmbH, Jena, Germany).

Flow Cytometry

Cells were detached from culture plates by trypsin, filtered through a 40 µm nylon mesh (BD Biosciences) to ensure single cellularity, re-suspended in ice-cold FACS buffer (PBS/1% bovine serum albumin) at 10^6 cells/200 µl and incubated for 20 minutes with antibodies against EpCAM, CD10, MUC1 and CD49f. To stain intercellular K5, cells were first surface-stained with anti-EpCAM and anti-CD49f antibodies, fixed with 4% paraformaldehyde at room temperature for 15 minutes, washed once with FACS buffer and once with FACS buffer containing 0.5 % saponin, and then incubated with anti-K5 antibody (1:100) in FACS buffer with saponin at room temperature for 30 minutes. Cells were then washed once in FACS buffer with saponin, once in FACS buffer before proceeding for flow cytometry analysis. Data were acquired on an LSRII (BD Biosciences) and analyzed using FlowJo software (Tree Star Inc., Ashland, OR, USA).

Immunoblotting assays

Cells were grown to 70-80% confluence in DFCI-I medium and starved of serum/growth factors in D3 medium [25] for 48 hours. For stimulation with EGFR ligands, starved cells were either left untreated or treated with 5 nM AREG, 5 nM EGF or 5 nM TGFα. After indicated stimulation period, cells were lysed in cold lysis buffer (0.5% Triton X-100, 50 mM Tris-HCl (pH 7.5), 150 mM sodium chloride, 1 mM phenylmethylsulfonyl fluoride, 1 mM sodium orthovanadate, and 10 mM sodium fluoride). Cell lysates were centrifuged at 10,000 rpm at 4 ºC for 30 min and protein concentrations in the supernatant was quantified using Bradford reagent (Bio-Rad, Richmond, CA, USA). Cell lysates (20 µg protein equivalent) were resolved by SDS-PAGE, transferred to polyvinylidene difluoride membranes (PerkinElmer Life Sciences, Waltham, MA, USA) and incubated with primary antibodies against pY (4G10), EGFR, pErk1/2, Erk1/2, pAkt, Akt or HSC70 followed by incubation with HRP-conjugated protein A (for rabbit antibodies) or rabbit anti-mouse antibody (for mouse monoclonal antibodies). Primary antibodies were diluted to 1:1000 in TBS-T (20 mM Tris-HCl (pH 8.0), 150 mM sodium chloride, and 0.1% v/v Tween-20), except anti-pY (4G10) which was used at 1:4000. Secondary antibodies were diluted to 1:25,000 in TBS-T. The enhanced chemiluminescence signals were recorded using a light-sensitive film (GeneMate Blue Lite Autorad Film).

Thymidine Incorporation Assay

Proliferation assay was performed essentially as described previously [26]. K5$^+$K19$^-$ hMEC cells were seeded in 24-well plates at 2×10^4/well in DFCI-1 medium. Next day, cells were rinsed and serum/growth factor-starved in D3 medium for 24 hours. Cells were then left unstimulated or stimulated with AREG, EGF or TGFα (all ligands at 5 nM) for 48 hours. [^{3}H] thymidine (4 µCi/ml) was added for the last 6 hours of incubation. To terminate incubations, unincorporated radioactivity was removed by washing cells once with ice-cold PBS followed by the addition of 10% trichloroacetic acid for 30 minutes at 4ºC. Next, wells were washed with ice-cold PBS and solubilized with 0.2 M NaOH at room temperature. The radioactivity was determined by liquid scintillation counting.

Statistical Analysis

Statistical analysis was performed using GraphPad Prism package (GraphPad Software, La Jolla, CA, USA).

Results

Characterization of *in vitro* differentiated K5$^+$K19$^-$ hMEC cells by flow cytometry

K5$^+$K19$^-$ hMEC cells maintain undifferentiated morphology and marker expression in DFCI-1 medium but they can be induced to differentiate towards both luminal and myoepithelial lineages when cultured in MEGM medium [12]. Original studies were carried out using immunofluorescence-based analyses. While this method is well-suited to correlate cell morphology, marker expression and its localization, objective quantitative assessment of individual markers require alternative approaches. Therefore, we sought to examine the differentiation process more quantitatively by flow cytometry.

To this end, K5$^+$K19$^-$ hMEC cells were cultured for three weeks in MEGM medium containing 5 nM EGF (see Materials and Methods for the detailed composition of this medium) and cell differentiation was examined by morphology, immunofluorescence and flow cytometry. In the DFCI-1 medium, all K5$^+$K19$^-$ hMEC cells maintained tightly-packed epithelial morphology (Figure 1A). In line with previous reports, all cells maintained in the DFCI-1 medium expressed

K5 and lacked MUC1 (Figure 1A). When analyzed by flow cytometry, most cells expressed intermediate to high levels of epithelial cell adhesion molecule (EpCAM) and high levels of integrin α6 (CD49f) (Figure 1B). On the other hand, when cultured in MEGM medium for three weeks, cells organized themselves into two distinct populations, one characterized by the tightly-packed epithelial morphology and the other spindle-shaped cells surrounding the tight epithelial colonies (Figure 1A). Spindle-shaped cells migrated away from the packed epithelial colonies even at low cell confluence while cells with epithelial morphology remained in the colonies even at high cell confluence. Changes in cell morphology were not the direct consequence of culture confluence. Immunofluorescence imaging revealed that spindle-shaped cells lost expression of K5 whereas a fraction of cells within the tightly-packed epithelial colonies expressed MUC1. MUC1^{pos} cells were found mostly in the center of the colonies. All these data are consistent with previous findings [12]. Flow cytometry analyses identified two distinct populations based on EpCAM expression (EpCAM^{hi} and EpCAM^{lo}) and EpCAM^{hi} cells could be further separated based on CD49f expression (CD49f^{hi}EpCAM^{hi} and CD49f^{lo}EpCAM^{hi}). Previous studies on normal primary hMECs reported that CD49f was expressed highly in stem/early progenitor cells while EpCAM was a marker for luminal lineage [27–30]. Therefore, we reasoned that EpCAM^{hi} population might be luminal cells that form tightly-packed colonies while EpCAM^{lo} population are spindle-shaped myoepithelial cells. To confirm this, we evaluated the expression of MUC1, a luminal marker, and CD10, a myoepithelial marker, in individual populations. As shown in Figure 1B, MUC1 was most highly expressed in the CD49f^{lo}EpCAM^{hi} population whereas CD10 expression was the highest in EpCAM^{lo} cells. To further establish the identity of each population, we sorted these three populations (Figure 1C) and subjected them to immunoblotting analysis for known markers of epithelial differentiation. The EpCAM^{lo} population lost K5 expression but up-regulated the expression of α-smooth muscle actin, a widely-accepted marker of myoepithelial differentiation. Changes in K5 expression was also confirmed by flow cytometry analysis (Figure S1). Altogether, we conclude that the tightly-packed epithelial colonies contain CD49f^{hi}EpCAM^{hi} and CD49f^{lo}EpCAM^{hi} cells, CD49f^{lo}EpCAM^{hi} population contains MUC1^{pos} cells, i.e., more differentiated luminal cells than CD49f^{hi}EpCAM^{hi} cells, and the surrounding spindle-shaped cells correspond to the EpCAM^{lo} population.

Effects of various EGFR ligands on K5$^+$K19$^-$ hMEC differentiation

Signals through EGFR play critical roles in mammary gland development and homeostasis. Seven different ligands have been identified for EGFR; EGF, amphiregulin (AREG), transforming growth factor alpha (TGFα), heparin-binding EGF-like growth factor (HB-EGF), betacelluin, epiregulin and epigen. They are known to differ in their binding affinity to EGFR, activate distinct biochemical pathways and have diverse effects on receptor trafficking, degradation and recycling [31,32]. Therefore, we sought to compare the effects of two other EGFR ligands relevant to mammary gland development and breast cancer, AREG and TGFα, on K5$^+$K19$^-$ hMEC cell differentiation.

To this end, K5$^+$K19$^-$ hMEC cells were cultured in modified MEGM medium where EGF was substituted with the same concentrations (5 nM) of AREG or TGFα. We selected this concentration because cells did not differentiate at lower concentrations of AREG (Figure S2). As shown in Figure 2A, there was no significant difference in cell growth when cells were maintained in MEGM medium containing AREG or TGFα from those cultured in the same medium containing EGF. However, cell acquired considerably different morphology under these conditions; specifically, almost all K5$^+$K19$^-$ hMEC cells cultured in the presence of AREG

formed tight epithelial colonies, and very few spindle-shaped cells were observed. In contrast, a majority of cells cultured in the presence of TGFα turned spindle-shape. These contrasting morphologies are reflected in the expression patterns of K5, MUC1, EpCAM, CD49f and CD10. AREG-treated cells maintained the expression of K5 and those in the middle of the colonies expressed MUC1 whereas a considerable fraction of TGFα-treated cells lost K5 expression and no MUC1-expressing cells were observed (Figure 2B). Flow cytometry analysis revealed the presence of a significant proportion of CD49f^{lo}EpCAM^{hi} (luminal) cells and very few EpCAM^{lo} (myoepithelial) cells when cultured with AREG, while most cells were EpCAM^{lo} (myoepithelial) when cultured in the presence of TGFα (Figure 2C). CD49f^{lo}EpCAM^{hi} (luminal) cells emerged in the presence of AREG were essentially indistinguishable from those emerged in the presence of EGF in that they maintained expression of K5 (as seen by immunofluorescence) and upregulated MUC1. Likewise, EpCAM^{lo} (myoepithelial) cells emerged in the presence of TGFα shared all the key characteristics with EGF-induced counterparts, i.e., they lost K5 expression and upregulated CD10. Altogether, we concluded that AREG-supplemented MEGM medium promoted the emergence of luminal cells whereas TGFα favored myoepithelial cells.

These results may indicate that different EGFR ligands, when administered as a part of MEGM medium, can directly regulate the lineage specification of K5^{+}K19^{-} hMEC cells. Alternatively, it is also conceivable that K5^{+}K19^{-} hMEC cells follow an intrinsic differentiation program and each EGFR ligand promotes the survival and/or proliferation of distinct populations. According to the latter hypothesis, AREG should preferentially promote the survival and/or proliferation of luminal cells, TGFα should support only myoepithelial cells while EGF should function both on luminal as well as myoepithelial cells. To test this hypothesis, we first evaluated the effects of various EGFR ligands on K5^{+}K19^{-} hMEC short-term cell growth. When undifferentiated K5^{+}K19^{-} hMEC cells were starved of serum/growth factors in D3 medium [25] and re-stimulated with EGF, AREG or TGFα, we did not detect significant difference in cell growth (Figure 3A). We next considered the possibility that each EGFR ligand may show preferential effects only on differentiated cells. To test this, we first allowed K5^{+}K19^{-} hMECs to differentiate *in vitro* in MEGM medium (containing EGF), sorted CD49f^{lo}EpCAM^{hi} (luminal) and EpCAM^{lo} (myoepithelial) populations by flow cytometry and cultured them in modified MEGM medium containing EGF, AREG or TGFα for 72 hours. Sorted cells maintained their morphology during this treatment (Figure S3). When cell proliferation was examined by the expression of the proliferation marker Ki67, the percentages of Ki67^{pos} (proliferating) cells were slightly reduced in CD49f^{lo}EpCAM^{hi} (luminal) cells treated with TGFα. Nevertheless, all three EGFR ligands supported proliferation of sorted cells (Figure 3B). Importantly, no significant cell death was observed either morphologically or by Annexin V staining throughout the course of differentiation in all three conditions (data not shown).

Combined with data that there was no significant difference in cell growth during three week differentiation (Figure 2A), these data collectively demonstrate that EGF, AREG and TGFα in MEGM medium show little difference in supporting growth and survival of K5^{+}K19^{-} hMEC cells either before or after *in vitro* differentiation, suggesting that the observed differences in K5^{+}K19^{-} hMEC differentiation in MEGM medium is not due to preferential survival and expansion of one population, but that EGFR ligands are likely to function directly on hMEC lineage specification in the context of this culture medium.

Biochemical consequences of EGFR engagement

To begin to dissect the mechanisms how different EGFR ligands regulate K5$^+$K19$^-$ hMEC cell fate, we first investigated short-term biochemical changes upon receptor engagement. In the present study, we focused on two major biochemical pathways downstream of EGFR, MEK-Erk and phosphatidylinositol 3-kinase (PI3K)-Akt pathways. K5$^+$K19$^-$ hMEC cells maintained in the DFCI-1 medium were starved for 48 hours in D3 medium. Cells were then stimulated with 5 nM of AREG, EGF or TGFα for up to 180 minutes (Figure 4). Consistent with the published literature [31,32], AREG induced little phosphorylation on EGFR and only a brief transient activation of Erk1/2. In contrast, TGFα and EGF induced significant phosphorylation of EGFR and sustained activation of Erk1/2. While EGF-induced Erk phosphorylation gradually declined after 45 minutes, TGFα-stimulated cells maintained a steady level of phosphorylated Erk up to 180 minutes. Similarly, both EGF and TGFα induced phosphorylation of Akt which lasted up to 90 minutes, whereas AREG stimulated cells showed little Akt phosphorylation. Furthermore, the levels of total EGFR declined rapidly after EGF stimulation and almost no EGFR was detected 90 minutes after stimulation, whereas TGFα-stimulated cells maintained a considerable amount of EGFR at the same time point. EGFR level remained unchanged upon AREG stimulation.

Differential effects of MEK and PI3K inhibition on differentiation of K5$^+$K19$^-$ hMEC cells

The biochemical analyses showed that both Erk and Akt were activated more robustly upon acute stimulation with EGF and TGFα than by AREG. To examine whether either of these pathways can directly regulate K5$^+$K19$^-$ hMEC differentiation, we performed *in vitro* differentiation assays in the presence of chemical inhibitors of MEK and PI3K. First, we cultured K5$^+$K19$^-$ hMECs in MEGM medium (containing EGF) for three weeks with a MEK inhibitor U0126 and examined differentiation by fluorescence microscopy and flow cytometry. Treatment with U0126 did not affect cell growth at the concentration tested (Figure S5). As shown in Figure 5B, K5$^+$K19$^-$ hMECs differentiated normally when treated with vehicle (DMSO) alone. However, cell differentiation was impaired in the presence of U0126. Specifically, significantly reduced number of spindle-shaped cells were observed around the tightly-packed epithelial clusters and essentially all cells maintained K5 expression. Flow cytometry confirmed that the percentages of both CD49f^{lo}EpCAM^{hi} and EpCAM^{lo} cells were markedly reduced compared to vehicle-treated cells. The efficacy of U0126 was confirmed by probing for inhibition of Erk activation (Figure 5A).

In contrast, when K5$^+$K19$^-$ hMECs were cultured in the presence of a PI3K inhibitor wortmannin, the emergence of differentiated (CD49f^{lo}EpCAM^{hi} and EpCAM^{lo}) cells was accelerated. As shown in Figure 5D, 10 days after cells were placed in MEGM medium when vehicle-treated cells have not differentiated yet, wortmannin-treated cells already showed morphological changes of differentiation and flow cytometry profiles were consistent with these observations. We confirmed similar effects with another PI3K inhibitor LY294002 (Figure S6).

From these data, we concluded that Erk activation, but not Akt activation, downstream of EGFR is required for differentiation of K5$^+$K19$^-$ hMECs in MEGM medium.

Discussion

Here we described an additional characterization of the h*TERT*-immortalized stem/progenitor K5$^+$K19$^-$ hMEC line *in vitro* differentiation model and its application to dissect biochemical mechanisms of MEC differentiation. By combining immunofluorescence microscopy, flow cytometry and biochemistry, we established that K5$^+$K19$^-$ hMECs, which express CD49f^{hi}EpCAM^{hi} under non-differentiating condition, differentiated into CD49f^{lo}EpCAM^{hi} and

EpCAM^{lo} cells. In the culture conditions examined here, this process can be regulated by signals through EGFR as demonstrated by distinct effects of EGFR ligands EGF, AREG and TGFα in MEGM medium. Downstream of EGFR, Erk activation is required to promote differentiation, whereas Akt activation counters this process.

Though activation of both Erk [33] and Akt [34] have been strongly tied to breast cancer, our knowledge into their precise roles in mammary gland development is not complete. Roles of Erk on cell fate determination were first investigated in the PC12 neural cell line. In this system, a transient activation of Erk was associated with cell proliferation while a more prolonged phosphorylation of Erk led to cell differentiation [35,36]. This concept was later extended to the mammary morphogenesis and lineage determination. Using primary mouse MECs, Fata et al. demonstrated that TGFα induced sustained activation of Erk and promoted branching morphogenesis whereas transient Erk activation by FGF7 promoted cell growth without branching [37]. In a comparable study using human cells, Pasic et al. showed that transient Erk activation by AREG promoted emergence of both luminal and myoepithelial cells while sustained Erk activation by EGF favored myoepithelial differentiation [23].

In the present study, we showed that the AREG-containing MEGM medium promoted luminal differentiation of K5^{+}K19^{-} hMECs while substitution with TGFα enhanced myoepithelial differentiation. Consistent with previous reports, stimulation with AREG induced transient Erk activation whereas more sustained activation was observed upon TGFα stimulation. Biochemical events from the acute phase of cell stimulation may not completely capture the continuously-unfolding changes in the complex signaling network over extended period required to induce cell differentiation. Nevertheless, effects of EGFR ligands on K5^{+}K19^{-} hMEC differentiation appear to be dependent on the MEK-Erk axis because chemical inhibition of this pathway, but not the PI3K-Akt pathway, interfered with this process. In addition, luminal differentiation appears to be less sensitive to MEK inhibition because the percentage of CD49f^{lo}EpCAM^{hi} (luminal) cells remained relatively unchanged while that of EpCAM^{lo} (myoepithelial) cells was reduced at lower concentrations of U0126 (Figure S4). Even at the highest concentration tested, a small number of MUC1^{pos} cells were repeatedly observed (Figure 5B). These results are essentially in agreement with findings by Pasic et al., which demonstrated that sustained activation of Erk through EGFR favored myoepithelial differentiation.

Nonetheless, some differences do exist in the spectrum of differentiated MECs between Pasic et al's results and the present study. Specifically, in the former, AREG promoted luminal as well as myoepithelial differentiation whereas EGF favored only myoepithelial differentiation. These differences may be due to that Pasic et al. utilized primary human MECs, which are intrinsically more heterogeneous than K5^{+}K19^{-} hMECs, which originated from a single clone [12]. Therefore, it is conceivable that their cell preparation contained progenitors capable of differentiating into both luminal and myoepithelial lineage upon AREG stimulation, whereas the K5^{+}K19^{-} hMECs originated from a clone which can only produce luminal cells with AREG. Additional differences in culture conditions between these studies include the presence of extracellular matrix and the composition of the base medium. Though previous studies demonstrated that h*TERT* alone could not transform MECs [38,39], its effects on MEC differentiation have not been fully clarified. These questions need to be addressed in future studies.

The PI3K-Akt axis has been shown to exert diverse effects on the normal and pathological development of mammary glands. In mice, loss of Akt1 inhibited, but loss of another family member Akt2 accelerated mammary tumorigenesis [40]. Conditional activation of this pathway

either through deletion of a negative regulator PTEN or over-expression of Akt induced precocious lactogenic differentiation of mammary epithelial cells [41,42]. These data apparently contradict our present findings that inhibition of the PI3K pathway accelerated differentiation of K5$^+$K19$^-$ hMECs.

However, activation of the PI3K-Akt pathway is also associated with the expansion of the mammary stem/progenitor populations and inhibition of differentiation [43]. Similar effects have been reported in other systems including embryonic stem cells [44] and neural stem cells [45]. One possible interpretation of these conflicting observations is that PIK3-Akt activity is required to maintain undifferentiated stem/progenitor state at the cell-autonomous level, but signals from tissue microenvironment can further modulate the ultimate outcome [46]. Collectively, our current results demonstrate that MEC differentiation is regulated by an intricate interplay between differentiation-promoting and -inhibiting signals, highlighting the complexity of the regulatory mechanisms of stem/progenitor cell maintenance and differentiation.

The biochemical and cell biological ramification of EGFR activation have been an object of extensive investigation. A number of studies demonstrated that AREG bound to EGFR with a much lower affinity than EGF, and while EGF-stimulated EGFR are internalized, ubiquitinated and degraded in the lysosome, receptor engagement with AREG or TGFα induced less degradation and more recycling [31,32]. Our preliminary investigation in K5$^+$K19$^-$ hMECs were consistent with published reports; a hundred (100) fold excess non-labeled AREG failed to displace fluorescence-labeled EGF, while excess non-labeled EGF or TGFα completely inhibited binding of labeled EGF (data not shown). All three ligands induced EGFR internalization at 5 nM within 10 minutes, but their intracellular fate differed significantly; EGFR trafficked to lysosomes and degraded upon EGF stimulation, whereas most EGFR recycled to the cell surface upon AREG stimulation (data not shown). In light of these observations, one possible interpretation of our present data is that the presence of low affinity EGFR ligand in MEGM medium promotes luminal differentiation and, as ligands bind with increasing affinity, cells begin to differentiate into myoepithelial lineage. This prompted us to examine whether lower concentrations of high affinity ligands mimic biological activity of low affinity ligands. However, when we cultured K5$^+$K19$^-$ hMECs in MEGM media containing varying concentrations of EGFR ligands, presence of lower concentrations of TGFα or EGF did not increase MUC1^{pos} cells, indicating that luminal differentiation was not augmented (Figure S2). Furthermore, though both AREG and TGFα are known to promote EGFR recycling rather than degradation, these ligands in MEGM medium showed opposing effects on K5$^+$K19$^-$ hMEC differentiation, AREG favoring luminal lineage and TGFα myoepithelial lineage. Altogether, present results indicate that biological consequences of EGFR engagement are not dictated by single factors such as receptor occupancy, binding affinity or receptor trafficking, but likely to be governed by the interaction of multiple determinants.

In conclusion, the present data validate the utility of the K5$^+$K19$^-$ hMEC cells for modeling key features of human MEC differentiation. We found that different EGFR ligands within MEGM medium could promote preferential differentiation into either luminal or myoepithelial fate. These findings open ways to dissect precise molecular/biochemical mechanisms of MEC differentiation, and we envision the K5$^+$K19$^-$ hMEC cells to be a useful model for this purpose.

Acknowledgements

References

1. Perou CM, Sørlie T, Eisen MB, Van de Rijn M, Jeffrey SS, et al. (2000) Molecular portraits of human breast tumours. Nature 406: 747–752. doi:10.1038/35021093.

2. Sørlie T, Perou CM, Tibshirani R, Aas T, Geisler S, et al. (2001) Gene expression patterns of breast carcinomas distinguish tumor subclasses with clinical implications. Proc Natl Acad Sci U S A 98: 10869–10874. doi:10.1073/pnas.191367098.

3. Sorlie T, Tibshirani R, Parker J, Hastie T, Marron JS, et al. (2003) Repeated observation of breast tumor subtypes in independent gene expression data sets. Proc Natl Acad Sci U S A 100: 8418–8423. doi:10.1073/pnas.0932692100.

4. Van Keymeulen A, Rocha AS, Ousset M, Beck B, Bouvencourt G, et al. (2011) Distinct stem cells contribute to mammary gland development and maintenance. Nature 479: 189–193. doi:10.1038/nature10573.

5. Van Amerongen R, Bowman AN, Nusse R (2012) Developmental stage and time dictate the fate of Wnt/β-catenin-responsive stem cells in the mammary gland. Cell Stem Cell 11: 387–400. doi:10.1016/j.stem.2012.05.023.

6. De Visser KE, Ciampricotti M, Michalak EM, Tan DW-M, Speksnijder EN, et al. (2012) Developmental stage-specific contribution of LGR5(+) cells to basal and luminal epithelial lineages in the postnatal mammary gland. J Pathol 228: 300–309. doi:10.1002/path.4096.

7. Lim E, Vaillant F, Wu D, Forrest NC, Pal B, et al. (2009) Aberrant luminal progenitors as the candidate target population for basal tumor development in BRCA1 mutation carriers. Nat Med 15: 907–913. doi:10.1038/nm.2000.

8. Proia TA, Keller PJ, Gupta PB, Klebba I, Jones AD, et al. (2011) Genetic predisposition directs breast cancer phenotype by dictating progenitor cell fate. Cell Stem Cell 8: 149–163. doi:10.1016/j.stem.2010.12.007.

9. Molyneux G, Geyer FC, Magnay F-A, McCarthy A, Kendrick H, et al. (2010) BRCA1 basal-like breast cancers originate from luminal epithelial progenitors and not from basal stem cells. Cell Stem Cell 7: 403–417. doi:10.1016/j.stem.2010.07.010.

10. Guo W, Keckesova Z, Donaher JL, Shibue T, Tischler V, et al. (2012) Slug and Sox9 Cooperatively Determine the Mammary Stem Cell State. Cell 148: 1015–1028. doi:10.1016/j.cell.2012.02.008.

11. Hennighausen L, Robinson GW (2005) Information networks in the mammary gland. Nat Rev Mol Cell Biol 6: 715–725. doi:10.1038/nrm1714.

12. Zhao X, Malhotra GK, Lele SM, Lele MS, West WW, et al. (2010) Telomerase-immortalized human mammary stem/progenitor cells with ability to self-renew and differentiate. Proc Natl Acad Sci U S A 107: 14146–14151. doi:10.1073/pnas.1009030107.

13. Sternlicht MD, Sunnarborg SW (2008) The ADAM17-amphiregulin-EGFR axis in mammary development and cancer. J Mammary Gland Biol Neoplasia 13: 181–194. doi:10.1007/s10911-008-9084-6.

14. Fowler KJ, Walker F, Alexander W, Hibbs ML, Nice EC, et al. (1995) A mutation in the epidermal growth factor receptor in waved-2 mice has a profound effect on receptor biochemistry that results in impaired lactation. Proc Natl Acad Sci U S A 92: 1465–1469.

15. Luetteke NC, Qiu TH, Fenton SE, Troyer KL, Riedel RF, et al. (1999) Targeted inactivation of the EGF and amphiregulin genes reveals distinct roles for EGF receptor ligands in mouse mammary gland development. Development 126: 2739–2750.

16. Nielsen TO, Hsu FD, Jensen K, Cheang M, Karaca G, et al. (2004) Immunohistochemical and clinical characterization of the basal-like subtype of invasive breast carcinoma. Clin Cancer Res 10: 5367–5374. doi:10.1158/1078-0432.CCR-04-0220.

17. Livasy CA, Karaca G, Nanda R, Tretiakova MS, Olopade OI, et al. (2006) Phenotypic evaluation of the basal-like subtype of invasive breast carcinoma. Mod Pathol 19: 264–271. doi:10.1038/modpathol.3800528.

18. Derynck R, Goeddel D V, Ullrich A, Gutterman JU, Williams RD, et al. (1987) Synthesis of messenger RNAs for transforming growth factors alpha and beta and the epidermal growth factor receptor by human tumors. Cancer Res 47: 707–712.

19. Bates SE, Davidson NE, Valverius EM, Freter CE, Dickson RB, et al. (1988) Expression of transforming growth factor alpha and its messenger ribonucleic acid in human breast cancer: its regulation by estrogen and its possible functional significance. Mol Endocrinol 2: 543–555.

20. Dotzlaw H, Miller T, Karvelas J, Murphy LC (1990) Epidermal growth factor gene expression in human breast cancer biopsy samples: relationship to estrogen and progesterone receptor gene expression. Cancer Res 50: 4204–4208.

21. LeJeune S, Leek R, Horak E, Plowman G, Greenall M, et al. (1993) Amphiregulin, epidermal growth factor receptor, and estrogen receptor expression in human primary breast cancer. Cancer Res 53: 3597–3602.

22. Qi CF, Liscia DS, Normanno N, Merlo G, Johnson GR, et al. (1994) Expression of transforming growth factor alpha, amphiregulin and cripto-1 in human breast carcinomas. Br J Cancer 69: 903–910.

23. Pasic L, Eisinger-Mathason TSK, Velayudhan BT, Moskaluk CA, Brenin DR, et al. (2011) Sustained activation of the HER1-ERK1/2-RSK signaling pathway controls myoepithelial cell fate in human mammary tissue. Genes Dev 25: 1641–1653. doi:10.1101/gad.2025611.

24. Band V, Sager R (1989) Distinctive traits of normal and tumor-derived human mammary epithelial cells expressed in a medium that supports long-term growth of both cell types. Proc Natl Acad Sci U S A 86: 1249–1253.

25. Band V, Zajchowski D, Kulesa V, Sager R (1990) Human papilloma virus DNAs immortalize normal human mammary epithelial cells and reduce their growth factor requirements. Proc Natl Acad Sci U S A 87: 463–467.

26. Maroni D, Davis JS (2011) TGFB1 disrupts the angiogenic potential of microvascular endothelial cells of the corpus luteum. J Cell Sci 124: 2501–2510. doi:10.1242/jcs.084558.

27. Stingl J, Eaves CJ, Zandieh I, Emerman JT (2001) Characterization of bipotent mammary epithelial progenitor cells in normal adult human breast tissue. Breast Cancer Res Treat 67: 93–109.

28. Clayton H, Titley I, Vivanco M dM (2004) Growth and differentiation of progenitor/stem cells derived from the human mammary gland. Exp Cell Res 297: 444–460. doi:10.1016/j.yexcr.2004.03.029.

29. Stingl J, Raouf A, Eirew P, Eaves CJ (2006) Deciphering the mammary epithelial cell hierarchy. Cell Cycle 5: 1519–1522.

30. Villadsen R, Fridriksdottir AJ, Rønnov-Jessen L, Gudjonsson T, Rank F, et al. (2007) Evidence for a stem cell hierarchy in the adult human breast. J Cell Biol 177: 87–101. doi:10.1083/jcb.200611114.

31. Roepstorff K, Grandal MV, Henriksen L, Knudsen SLJ, Lerdrup M, et al. (2009) Differential effects of EGFR ligands on endocytic sorting of the receptor. Traffic 10: 1115–1127. doi:10.1111/j.1600-0854.2009.00943.x.

32. Baldys A, Göoz M, Morinelli TA, Lee M-H, Raymond JR, et al. (2009) Essential role of c-Cbl in amphiregulin-induced recycling and signaling of the endogenous epidermal growth factor receptor. Biochemistry 48: 1462–1473. doi:10.1021/bi801771g.

33. Whyte J, Bergin O, Bianchi A, McNally S, Martin F (2009) Key signalling nodes in mammary gland development and cancer. Mitogen-activated protein kinase signalling in experimental models of breast cancer progression and in mammary gland development. Breast Cancer Res 11: 209. doi:10.1186/bcr2361.

34. Wickenden JA, Watson CJ (2010) Key signalling nodes in mammary gland development and cancer. Signalling downstream of PI3 kinase in mammary epithelium: a play in 3 Akts. Breast Cancer Res 12: 202. doi:10.1186/bcr2558.

35. Qui MS, Green SH (1992) PC12 cell neuronal differentiation is associated with prolonged p21ras activity and consequent prolonged ERK activity. Neuron 9: 705–717.

36. Traverse S, Gomez N, Paterson H, Marshall C, Cohen P (1992) Sustained activation of the mitogen-activated protein (MAP) kinase cascade may be required for differentiation of PC12 cells. Comparison of the effects of nerve growth factor and epidermal growth factor. Biochem J 288 (Pt 2: 351–355.

37. Fata JE, Mori H, Ewald AJ, Zhang H, Yao E, et al. (2007) The MAPK(ERK-1,2) pathway integrates distinct and antagonistic signals from TGFalpha and FGF7 in morphogenesis of mouse mammary epithelium. Dev Biol 306: 193–207. doi:10.1016/j.ydbio.2007.03.013.

38. Hahn WC, Counter CM, Lundberg AS, Beijersbergen RL, Brooks MW, et al. (1999) Creation of human tumour cells with defined genetic elements. Nature 400: 464–468. doi:10.1038/22780.

39. Elenbaas B (2001) Human breast cancer cells generated by oncogenic transformation of primary mammary epithelial cells. Genes Dev 15: 50–65. doi:10.1101/gad.828901.

40. Maroulakou IG, Oemler W, Naber SP, Tsichlis PN (2007) Akt1 ablation inhibits, whereas Akt2 ablation accelerates, the development of mammary adenocarcinomas in mouse mammary tumor virus (MMTV)-ErbB2/neu and MMTV-polyoma middle T transgenic mice. Cancer Res 67: 167–177. doi:10.1158/0008-5472.CAN-06-3782.

41. Li G, Robinson GW, Lesche R, Martinez-Diaz H, Jiang Z, et al. (2002) Conditional loss of PTEN leads to precocious development and neoplasia in the mammary gland. Development 129: 4159–4170.

42. Chen C-C, Stairs DB, Boxer RB, Belka GK, Horseman ND, et al. (2012) Autocrine prolactin induced by the Pten-Akt pathway is required for lactation initiation and provides a direct link between the Akt and Stat5 pathways. Genes Dev 26: 2154–2168. doi:10.1101/gad.197343.112.

43. Korkaya H, Paulson A, Charafe-Jauffret E, Ginestier C, Brown M, et al. (2009) Regulation of Mammary Stem/Progenitor Cells by PTEN/Akt/β-Catenin Signaling. PLoS Biology 7: e1000121. doi:10.1371/journal.pbio.1000121.

44. Watanabe S, Umehara H, Murayama K, Okabe M, Kimura T, et al. (2006) Activation of Akt signaling is sufficient to maintain pluripotency in mouse and primate embryonic stem cells. Oncogene 25: 2697–2707. doi:10.1038/sj.onc.1209307.

45. Groszer M, Erickson R, Scripture-Adams DD, Lesche R, Trumpp A, et al. (2001) Negative regulation of neural stem/progenitor cell proliferation by the Pten tumor suppressor gene in vivo. Science 294: 2186–2189. doi:10.1126/science.1065518.

46. Venere M, Lathia JD, Rich JN (2013) Growth Factor Receptors Define Cancer Hierarchies. Cancer Cell 23: 135–137. doi:10.1016/j.ccr.2013.01.020.

Tables

Table 1. List of antibodies used for this study.

	Vendor	Clone Name	Catalog Number
Phosphotyrosine	EMD Millipore	4G10	05-321
EGFR	Santa Cruz Biotechnology	Rabbit polyclonal	sc-03
Phospho-p44/42 MAPK (Erk1/2) (Thr202/Tyr204)	Cell Signaling Technology	Rabbit polyclonal	9101
p44/42 MAPK (Erk1/2)	Cell Signaling Technology	Rabbit polyclonal	9102
Phospho-Akt (Ser473)	Cell Signaling Technology	D9E	4060
Akt	Cell Signaling Technology	C67E7	4691
HSC70	Santa Cruz Biotechnology	B-6	sc-7298
MUC1	BD Biosciences	HMPV	550486
MUC1-FITC	BD Biosciences	HMPV	559774
EpCAM-APC	BD Biosciences	EBA-1	347200
CD49f-PE-Cy7	eBioscience	eBioGoH3	25-0495
CD10-APC eFluor 780	eBioscience	SN5c	8047-0108
Cytokeratin 5	Covance	Rabbit polyclonal	PRB-160P
Cytokeratin 5/6-FITC	EMD Millipore	D5/16B	FCMAB291F
Alpha Smooth Muscle Actin	Sigma-Aldrich	1A4	A2547
HRP-Protein A	Invitrogen	N/A	10-1023
HRP-Rabbit anti-Mouse IgG (H+L) conjugate	Invitrogen	Rabbit polyclonal	R21455
Alexa Fluor 488 Donkey anti-Rabbit IgG (H+L)	Invitrogen	Donkey polyclonal	A-21206
Alexa Fluor 594 Donkey anti-Mouse IgG (H+L)	Invitrogen	Donkey polyclonal	A-21203

Figure Legends

Figure 1. In vitro differentiation of K5$^+$K19$^-$ h*TERT*-immortalized mammary epithelial cells.

Cells were either maintained under non-differentiating condition (DFCI-1 medium) or propagated under differentiation-promoting condition (MEGM medium containing 5 nM EGF) for three weeks and cell morphology and marker expressions were evaluated. Shown are representative results from more than 10 independent experiments with similar outcome. **(A)** Overall cell morphology was assessed by Wright-Giemsa staining (top panels) and K5 (green) and MUC1 (purple) expression was assessed by immunofluorescence microscopy (bottom panels). Nuclei were visualized with DAPI (blue). Red bars indicate 50 µM. **(B)** Expression of CD49f, EpCAM, MUC1 and CD10 was assessed by flow cytometry. Gates for CD49f^{lo}EpCAM^{hi} (luminal, green box), EpCAM^{lo} (myoepithelial, red box) and CD49f^{hi}EpCAM^{hi} (undifferentiated, black box) cells are indicated. Histograms on the right indicate levels of MUC1 (luminal marker, top) and CD10 (myoepithelial marker, bottom) in cells propagated in MEGM medium. Green lines represent the levels of MUC1 (top) or CD10 (bottom) in the CD49f^{lo}EpCAM^{hi} (luminal) population, red lines are for the EpCAM^{lo} (myoepithelial) population and black lines for the CD49f^{hi}EpCAM^{hi} (undifferentiated) population. **(C)** Expression of α-smooth muscle actin (αSMA) and K5 was assessed by immunoblotting. NIH3T3 cells (lane 1) were included as a positive control for αSMA. Lane 2: K5$^+$K19$^-$ hMECs maintained in DFCI-1 medium; Lanes 3-5: K5$^+$K19$^-$ hMECs were differentiated in MEGM medium and sorted into CD49f^{lo}EpCAM^{hi} (luminal), EpCAM^{lo} (myoepithelial) and CD49f^{hi}EpCAM^{hi} (undifferentiated) populations. Membrane was probed for HSC70 to ensure equal loading.

Figure 2. Effects of various EGFR ligands on K5$^+$K19$^-$ hMEC differentiation in MEGM medium.

Cells were propagated in modified MEGM media where EGF was substituted with either AREG or TGFα and morphology and marker expressions were analyzed after three weeks. **(A)** Cell growth during differentiation. Two hundred thousand (2 x 10^5) K5$^+$K19$^-$ hMECs were seeded in 60 mm dishes in modified MEGM media with indicated EGFR ligands. Cell numbers were determined every week. Shown are averages from 4 independent experiments. Error bars indicate standard errors. There was no statistically significant difference between groups in cell number at each time point by one-way ANOVA with Bonferroni multiple comparisons. **(B)** Overall cell morphology was assessed by Wright-Giemsa staining (left panels) and K5 (green) and MUC1 (purple) expression was assessed by immunofluorescence microscopy (right panels). Nuclei were visualized with DAPI (blue). Red bars indicate 50 µM. **(C)** Expression of CD49f, EpCAM, MUC1 and CD10 was analyzed by flow cytometry. Gates and percentages for CD49f^{lo}EpCAM^{hi} (luminal, green box), EpCAM^{lo} (myoepithelial, red box) and CD49f^{hi}EpCAM^{hi} (undifferentiated, black box) populations are indicated in the top panels. Middle and bottom panels are histograms for MUC1 (middle) and CD10 (bottom). Green lines represent the levels of MUC1 (middle) or CD10 (bottom) in the CD49f^{lo}EpCAM^{hi} (luminal) population, red lines are for the EpCAM^{lo} (myoepithelial) population and black lines for the CD49f^{hi}EpCAM^{hi} (undifferentiated) population. Histograms for EpCAM^{lo} (myoepithelial) populations in AREG-treated cells and CD49f^{lo}EpCAM^{hi} (luminal) and CD49f^{hi}EpCAM^{hi} (undifferentiated) populations in TGFα-treated are not shown in the overlays due to extremely small cell numbers. Though the difference in MUC1 expression between EGF-treated cell populations was not as robust as in Figure 1B in

this particular experiment, MUC1 mean fluorescence intensity for CD49f^{lo}EpCAM^{hi} (luminal) cells (642) was higher than that of EpCAM^{lo} (myoepithelial) or CD49f^{hi}EpCAM^{hi} (undifferentiated) cells (437 and 337, respectively). **(B)** and **(C)** are representative results from 6 independent experiments with similar outcome.

Figure 3. All EGFR ligands support growth of K5$^+$K19$^-$ hMECs before and after differentiation.

(A) Undifferentiated K5$^+$K19$^-$ hMECs were starved of serum/growth factors for 24 hours in D3 medium before being left unstimulated (Control) or stimulated with AREG, EGF or TGFα (all at 5 nM) for 24 hours. Cell growth was assessed by [^{3}H] thymidine incorporation for the last 6 hours of incubation. A representative result from 2 independent experiments run in triplicates is shown. Error bars indicate standard errors. **(B)** K5$^+$K19$^-$ hMECs were propagated in MEGM medium (with EGF) to induce differentiation. Differentiated luminal (CD49f^{lo}EpCAM^{hi}) and myoepithelial (EpCAM^{lo}) cells were separated by FACS and plated in modified MEGM medium containing either AREG, EGF or TGFα (all at 5 nM). The percentage of proliferating cells was assessed by the expression of Ki67. Each condition was run in 5 replicates. Error bars represent standard errors. The difference between EGF and TGFα, as well as that between AREG and TGFα in CD49f^{lo}EpCAM^{hi} cells was statistically significant at p<0.05 when analyzed by one-way ANOVA with Bonferroni multiple comparisons.

Figure 4. Biochemical consequences of EGFR engagement with various ligands.

Undifferentiated K5$^+$K19$^-$ hMECs were starved of serum/growth factors for 48 hours in D3 medium before being stimulated with 5 nM EGF, AREG or TGFα for indicated period. Cell lysate was analyzed by immunoblotting. **(A)** Immunoblot results of phosphotyrosine (p-Tyr), total EGFR, phospho-p44/42 MAPK (p-Erk1/2), total p44/42 MAPK (Erk1/2), phospho-Akt (p-Akt) and total Akt. HSC70 was used as loading control. A representative of 2 independent experiments is shown. **(B)** Results from 2 independent experiments were quantitated by densitometry and ratios of p-Erk/total Erk and p-Akt/total Akt were plotted. Shown are averages of 2 experiments; error bars indicate standard errors. Y axis is in arbitrary unit.

Figure 5. MEK inhibitor blocks differentiation of K5$^+$K19$^-$ hMECs.

(A) Undifferentiated K5$^+$K19$^-$ hMECs were starved of serum/growth factors for 48 hours in D3 medium, treated with 1 µM U0126 or vehicle (DMSO) alone for 4 hours before stimulation with 5 nM EGF for the indicated period. Cell lysate was analyzed by immunoblotting. **(B)** K5$^+$K19$^-$ hMECs were propagated in MEGM medium (containing EGF) with or without 1 µM U0126 for three weeks. Medium was replaced every two days. Overall cell morphology was assessed by Wright-Giemsa staining (top panels) and K5 (green) and MUC1 (red) expression was assessed by immunofluorescence microscopy (middle panels). Nuclei were visualized with DAPI (blue). Red bars indicate 50 µM. Expression of CD49f and EpCAM was analyzed by flow cytometry (bottom panels). Gates and percentages for CD49f^{lo}EpCAM^{hi} (luminal, green box) and EpCAM^{lo} (myoepithelial, red box) populations are indicated. Shown are representative results from 3 independent experiments. **(C)** Undifferentiated K5$^+$K19$^-$ hMECs were starved of serum/growth factors for 48 hours in D3 medium, treated with 5 µM wortmannin or vehicle (DMSO) alone for 4 hours before stimulation with 5 nM EGF for the indicated period. Cell lysate was analyzed by immunoblotting. **(D)** K5$^+$K19$^-$ hMECs were propagated in MEGM medium (containing EGF) with or without 5 µM wortmannin for ten days. At this time point, control culture has not differentiated yet. Medium was replaced every two days. Overall cell morphology was assessed

by Wright-Giemsa staining (top panels) and K5 (green) and MUC1 (red) expression was assessed by immunofluorescence microscopy (middle panels). Nuclei were visualized with DAPI (blue). Red bars indicate 50 µM. Expression of CD49f and EpCAM was analyzed by flow cytometry (bottom panels). Gates and percentages for CD49f^{lo}EpCAM^{hi} (luminal, green box) and EpCAM^{lo} (myoepithelial, red box) populations are indicated. Shown are representative results from 2 independent experiments.

Supporting Information Legends

Figure S1. Expression of K5 after differentiation.

Cells were either maintained under non-differentiating condition (DFCI-1 medium) or propagated under differentiation-promoting condition (MEGM medium containing 5 nM EGF) for three weeks and expression of CD49f, EpCAM and K5 was assessed by flow cytometry. Cells were fixed and permeabilized for intracellular K5 staining. Gates for CD49f^{lo}EpCAM^{hi} (luminal, green box), EpCAM^{lo} (myoepithelial, red box) and CD49f^{hi}EpCAM^{hi} (undifferentiated, black box) cells are indicated. Note that CD49f and EpCAM expression patterns are slightly altered compared to those in Figures 1, 2 and 5 due to cell fixation and permeabilization. Histograms indicate levels of K5 in cells propagated in MEGM medium. The green line represents the levels of K5 in the CD49f^{lo}EpCAM^{hi} (luminal) population, the red line is for the EpCAM^{lo} (myoepithelial) population and the black line for the CD49f^{hi}EpCAM^{hi} (undifferentiated) population. Mean fluorescence intensity of K5 for CD49f^{lo}EpCAM^{hi} (luminal), EpCAM^{lo} (myoepithelial) and CD49f^{hi}EpCAM^{hi} (undifferentiated) populations are 1802, 806 and 1695, respectively.

Figure S2. Effect of varying doses of EGFR ligands in MEGM medium on MEC differentiation.

K5^{+}K19^{-} hMECs were propagated in modified MEGM medium containing indicated concentrations of EGFR ligands EGF, AREG or TGFα for three weeks. Cell differentiation was evaluated by K5 (green) and MUC1 (purple) staining. Nuclei were visualized with DAPI (blue). Red bars indicate 50 µM.

Figure S3. Cell morphology after sort.

K5^{+}K19^{-} hMECs were propagated in MEGM medium (containing EGF) for three weeks and sorted based on CD49f and EpCAM expression. Sorted CD49f^{lo}EpCAM^{hi} (luminal) and EpCAM^{lo} (myoepithelial) populations cells were seeded into modified MEGM medium where EGF was substituted with AREG or TGFα. Cell morphology was documented three days later.

Figure S4. Effect of varying doses of MEK inhibitor on differentiation.

K5^{+}K19^{-} hMECs were propagated in MEGM medium (containing EGF) with indicated concentrations of U0126 for three weeks. Medium was replaced every two days. Expression of CD49f and EpCAM was analyzed by flow cytometry. Gates and percentages for CD49f^{lo}EpCAM^{hi} (luminal, green box) and EpCAM^{lo} (myoepithelial, red box) populations are indicated.

Figure S5. Effect of U0126 and wortmannin on cell growth.

K5^{+}K19^{-} hMECs were seeded in MEGM medium (with 5 nM EGF) in 6 well plates at 10^{4} cells/well and effects of U0126 and wortmannin on cell growth were evaluated. Cells were

detached from plates at indicated time points and live cell numbers were determined. Shown are average cell numbers from 6 replicates. Error bars indicate standard errors. There was no statistically significant difference between DMSO and U0126 treatment groups; Wortmannin treatment significantly inhibited cell growth.

Figure S6. Effect of LY294002 on differentiation.

K5$^+$K19$^-$ hMECs were cultured in MEGM medium (containing EGF) for 8 days in the presence or absence of 0.5 µM LY294002 and cell differentiation was evaluated by flow cytometry.

Figure 1

Figure 2

A

B

Figure 3

Figure 4

A

DMSO control | U0126 (1 µM)

EGF (5nM): − + + − + +
Time (min): 0 10 30 0 10 30

p-Erk1/2
Erk1/2
HSC70

C

DMSO control | Wortmannin (5 µM)

EGF (5nM): − + + − + +
Time (min): 0 10 30 0 10 30

p-Akt
Akt
HSC70

B

DMSO control | U0126 (1 µM)

Wright-Giemsa

K5 MUC1 DAPI

EpCAM vs CD49f

13.5 / 19.8 | 5.86 / 1.03

D

DMSO control | Wortmannin (5 µM)

Wright-Giemsa

K5 MUC1 DAPI

EpCAM vs CD49f

1.03 / 1.32 | 20.9 / 11.4

Figure 5

Figure S1

	0.05 nM	0.5 nM	5 nM
EGF			K5 MUC1 DAPI
AREG			K5 MUC1 DAPI
TGFα			K5 MUC1 DAPI

Figure S2

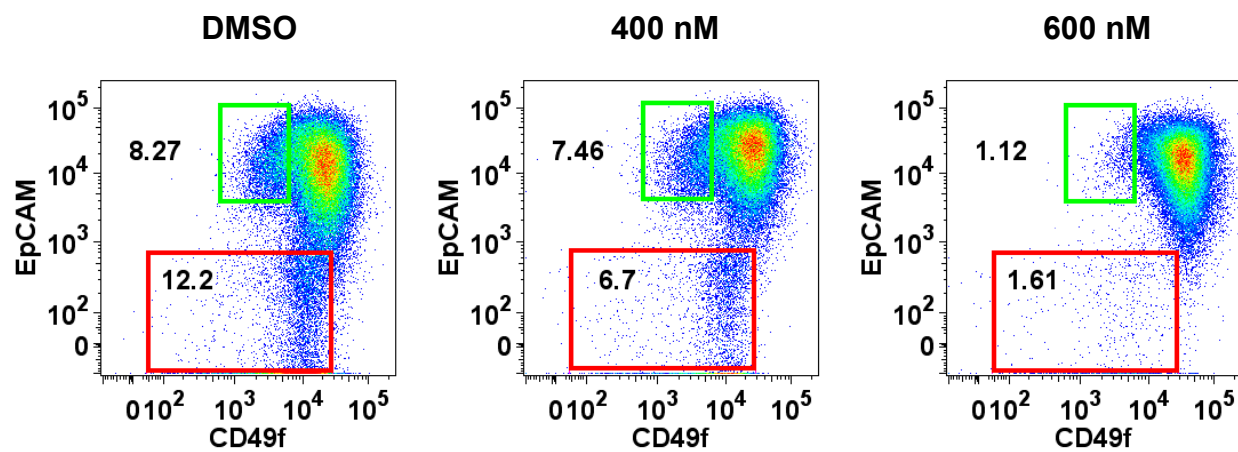**CD49f^{lo}EpCAM^{hi} (Luminal)**   **EpCAM^{lo} (Myoepithelial)**

EGF

AREG

TGFα

Figure S3

Figure S4

Figure S5

DMSO **LY294002 (0.5 µM)**

Figure S6